Phase identification of micro and macro bubbles at the interface of directly bonded GaAs on sapphire

ST. SENZ, P. KOPPERSCHMIDT, G. KÄSTNER, D. HESSE
Max-Planck-Institut für Mikrostrukturphysik, Weinberg 2, D-06120 Halle (Saale), Germany

Direct wafer bonding (DWB) of 3″ GaAs and R-cut sapphire was performed in a microcleanroom using ultra pure water as cleaning agent. The initial bonding is mediated by Van der Waals forces and hydrogen bridges. The bond energy is released by subsequent heating up to temperatures of 500 °C. During heating the formation of macroscopic bubbles at the interface was observed. Details of the interface structure were investigated by cross-sectional as well as plan-view transmission electron microscope (TEM) micrographs. The chemical composition of the elements at the interface was measured by energy dispersive X-ray analysis (EDX) and electron energy loss spectroscopy (EELS). A high density of micro bubbles in bonded areas, a network of micro channels in the transition region and macro bubbles in debonded areas could be distinguished. The macro bubbles are filled with a porous oxide. X-ray diffraction (XRD) and selected area electron diffraction (SAED) revealed the growth of textured γ-Ga_2O_3 and elemental arsenic. © *1998 Chapman & Hall*

1. Introduction

Direct wafer bonding (DWB) is a method to join different materials, independent of their crystallography, lattice misorientation and chemical structure [1, 2]. Two mirror-polished wafers are cleaned by deionized and filtered water and dried by rotation in a microcleanroom [3]. The wafers are then brought into contact face to face at room temperature. The usual spontaneous initial bonding is mediated by attractive Van der Waals forces and hydrogen bridges between the surface atoms. Subsequent heating at several hundred degrees centigrade is used to increase the bond energy up to values comparable to the energy of atomic bonds in the bulk material. DWB enables the fabrication of many material combinations which previously were not accessible.

Many applications of DWB are in the field of the silicon on insulator (SOI) technology [2, 4, 5]. Within recent years production processes implementing DWB for vertical cavity surface emitting lasers (VCSEL) [6, 7], acceleration and pressure sensors [8] as well as for optoelectronic integrated circuits (OEICs) [9] were developed.

The interest in gallium arsenide-based electronic devices increased recently because of demand from the communication industry for high frequency devices. DWB using GaAs substrates was first reported in 1988 [11]. The fabrication of bonded pairs of lattice-mismatched wafers (InP and GaAs) has been demonstrated for the first time in 1990 [12]. DWB plays an increasing role when combining GaAs with silicon substrates. A major difficulty in using DWB for the combination of these materials is the difference in their thermal expansion coefficients by a factor of about 2 [13].

Direct bonding of GaAs on sapphire, a combination useful for hybrid devices in the range of microwave frequencies, was introduced by Kopperschmidt *et al.* [14]. Due to the very similar coefficient of thermal expansion of GaAs and sapphire this particular material combination is well suited for the DWB approach. However, as a major drawback it turned out that during annealing the bonded GaAs/sapphire wafer pair, macroscopic bubbles, microscopic bubbles and a network of micro channels were observed which are investigated in this paper using transmission electron microscopy (TEM) methods including electron energy loss spectroscopy (EELS) and X-ray diffraction (XRD).

2. Experimental procedure

Wafers with low surface roughness of a polishing quality declared by the supplier as "for epitaxy" were used. A semi-insulating 3″ (1 0 0) GaAs wafer was positioned face to face to a 3″ R-cut sapphire wafer in a microcleanroom [3]. The wafers were separated by three small spacers and first cleaned by rinsing with deionized and thoroughly filtered water for several minutes. Then the microcleanroom was closed and the wafers were dried by rotating at 3300 r.p.m. for 5–7 min. The wafers were heated by an infrared lamp to accelerate drying. The bonding process was simply initiated by removing the spacers and dropping the

upper wafer onto the lower one. After applying a local pressure the bond front started at a nucleation site and spread over the whole wafer pair. A subsequent annealing at 500 °C for 5 h increased the bond energy up to the energy of atomic bonds in the bulk material. High bond energies up to $3\ \mathrm{J\,m^{-2}}$ were measured by the crack opening method [15]. During this heating the wafer pair was monitored with reflected light through a viewpoint. The growth of gas-filled bubbles was observed above 95 °C. The high bond strength enabled the preparation of TEM cross-sections of the bonded interface for structural and morphological investigations.

TEM cross-sections were prepared in the conventional way by cutting, grinding, polishing and finally ion beam thinning. A Philips transmission electron microscope CM 20 twin (200 kV, point resolution 0.27 nm) with a Ge-detector for EDX was used for TEM work. Composition analysis with high lateral resolution (<3 nm) was done with a Philips CM 20 FEG equipped with EDX and parallel EELS. High resolution images were taken with a Jeol 4000 EX (400 kV, point resolution 0.19 nm). X-ray diffraction and pole figure measurements were performed with a Philips X'Pert MRD. The diffracted radiation was detected with a parallel plate collimator (2θ resolution 0.35°) and a graphite secondary monochromator selecting the $\mathrm{CuK_\alpha}$ line.

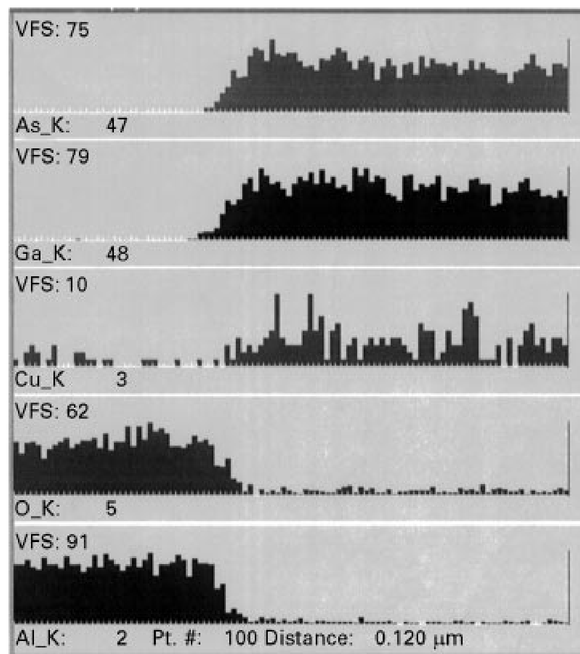

Figure 2 EDX linescan across the interface GaAs to sapphire. The copper signal results from the specimen supporting ring.

3. Results and discussion

3.1. Micro bubbles

A bonded area was checked first by an ultrasonic microscope and showed no visible defects. In Fig. 1 a cross-sectional high resolution TEM picture of the two lattices at the interface and one micro bubble are shown. The electron beam was parallel to the GaAs direction [0 1 1]. The cross-section reveals intimate contact of the lattices within less than 1 nm. Fig. 2 shows an EDX linescan across the interface at a position free from voids or bubbles. No evidence for interdiffusion or chemical reaction was observed.

Along the interface micro bubbles, 3–10 nm in depth and 10–20 nm in width, of the type shown in Fig. 1 were frequently found. Their boundaries were $\langle 1\,1\,1\rangle$ and $\langle 1\,0\,0\rangle$ oriented. They were filled with amorphous and polycrystalline material. Fig. 3 shows EELS point analyses along the interface. Fig. 3a depicts an arsenic-rich and oxygen-free bubble, decorated by copper during the thinning process in the ion beam milling equipment. (All cross-sectional specimens were stabilized by glueing them to a copper support ring.) An example of a void filled with a slightly gallium-rich GaAs and a weak signal from oxygen is shown in Fig. 3b. The main result of EDX and EELS measurements was the absence of elements other than Al, O, Ga and As at the interface. The content of the bubbles was mainly GaAs, but the ratio deviated towards gallium- or arsenic-rich compositions. The micro bubbles were not filled with a fully oxidized material; the weak oxygen count rate can be explained by the neighbouring Al_2O_3. Since hydrogen is not detectable by EDX, EELS measurements were performed. No evidence for hydrides or hydroxides was found. However, the sensitivity was not sufficient to exclude such compounds.

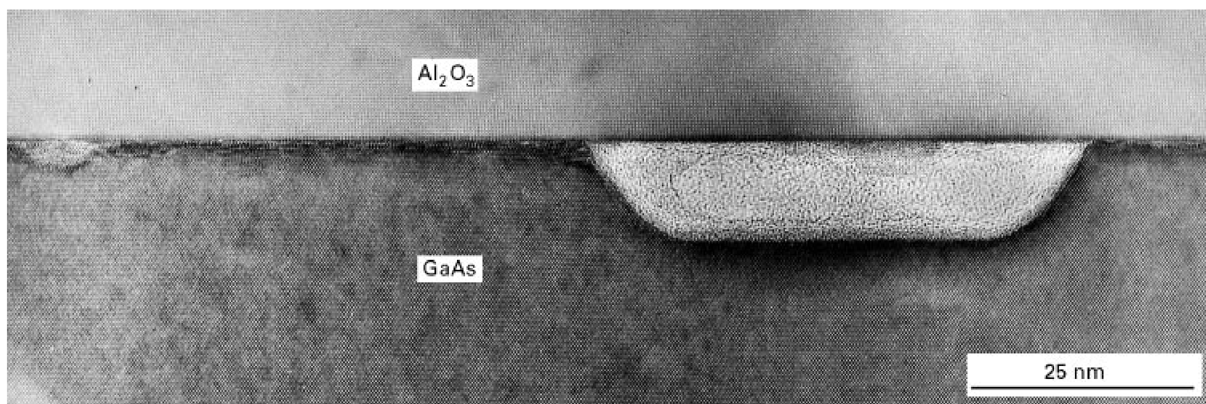

Figure 1 HREM cross section image of the interface GaAs to sapphire, showing a large micro bubble. The direction of the electron beam is parallel to [0 1 1] GaAs.

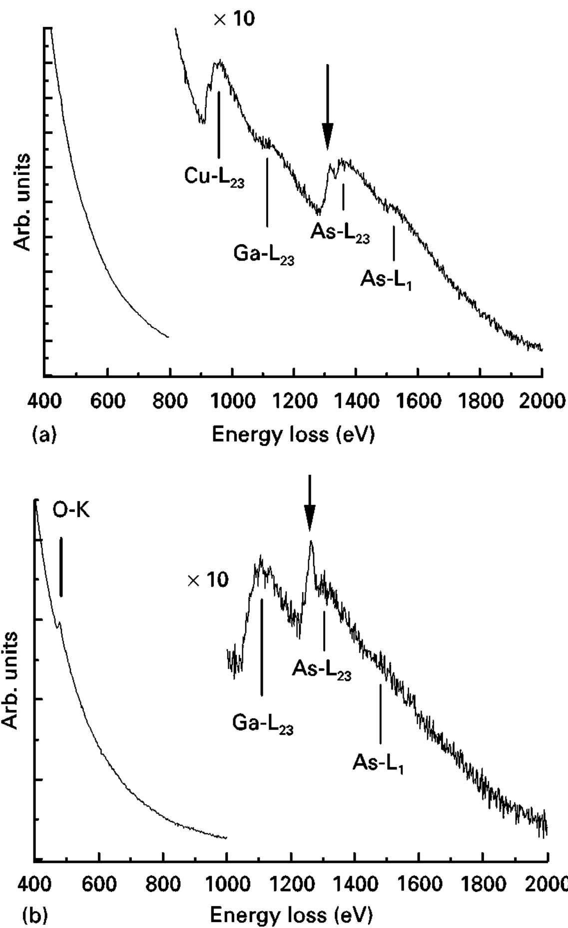

Figure 3 EELS point analyses at interface inhomogeneities near the interface GaAs to sapphire. The arrow marks a spurious response by stray electrons.

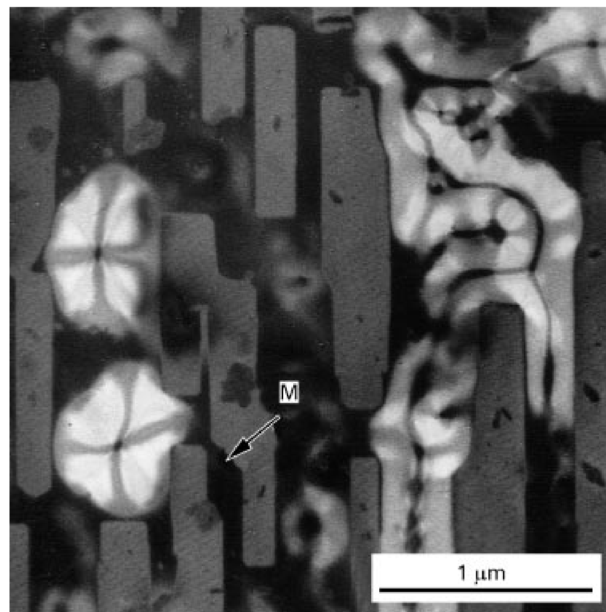

Figure 4 TEM plan-view image of an area with a micro channel network.

Planar TEM specimens were prepared parallel to the bonded interface to check the lateral distribution of possible defects in the interface. We found numerous small inhomogeneities of about 30 nm in diameter, separated by a mean distance of about 500 nm. They correspond to the micro bubbles visible in the cross section shown above. An example of a micro channel network in the vicinity of a macro bubble is shown in Fig. 4. The bonded areas of uniform grey contrast show fine Moiré fringes running parallel to M. They are separated by micro channels, where the diffraction contrast reveals strong bending contours. Their fourfold symmetry indicates a locally bell-shaped lattice. The origin of this bending might be high stress or internal pressure.

3.2. Macro bubbles

At some areas the wafers debonded after the heat treatment, forming bubbles of macroscopic size, featuring lateral dimensions in the range of mm to cm. The solid state content of these macro bubbles was accessible after cutting away the sapphire wafer. To identify any possible oriented phases, XRD pole figures were measured for a number of different 2θ settings. The only crystalline and oriented phases identified by this procedure were γ-Ga_2O_3 and elemental arsenic.

Figs 5 and 6 show XRD pole figures measured with the planes $\{1\,1\,3\}$ of γ-Ga_2O_3 ($2\theta = 36°$; Fig. 5) and $\{0\,1\,2\}$ of hexagonal arsenic ($2\theta = 32.4°$; Fig. 6). γ-Ga_2O_3 crystallizes in a cubic spinel structure with a high density of defects. The 2θ full width half maximum (FWHM) of the oxide reflections was around 2°. This high value might be a result of the comparatively low formation temperature. XRD pole figure analysis allows the detection of oriented phases with a high sensitivity. The count rate for a well-oriented crystalline material is enhanced by a factor of 1000 to 10 000 relative to a polycrystalline sample. The γ-Ga_2O_3 has a relatively broad tilting and in-plane rotation distribution, while the arsenic shows narrow peaks of different orientation relationships.

Fig. 7 shows a TEM bright-field image of a cross-section, and Fig. 8 the corresponding electron diffraction image. The electron diffraction image is dominated by the textured phase γ-Ga_2O_3 and sharp spots from GaAs. Additional weak polycrystalline rings do not fit to the known Ga–As–O phases. The chemical composition of the porous film was measured by EDX (Ga 84%, As 16%, oxygen). EDX is not sensitive to hydrogen, thus we can not exclude either an incorporation of water in the crystal structure or the formation of hydroxides.

The porous structure of the oxide film is obviously a result of As losses during heating and oxidation. The gas AsH_3 might have formed during the reaction of the water at the interface with GaAs to the stable oxide γ-Ga_2O_3. AsH_3 is unstable and dissociates above 230 °C. At higher temperatures arsenic and its oxides are volatile [10] and are easily redistributed during the prolonged heating period.

Oxidation of GaAs under normal or low pressure at temperatures of several hundred degrees centrigrade leads to the formation of β-Ga_2O_3 [10]. Mitani and Gösele [16] discussed a thermodynamic model for the formation of bubbles at the interface of bonded silicon

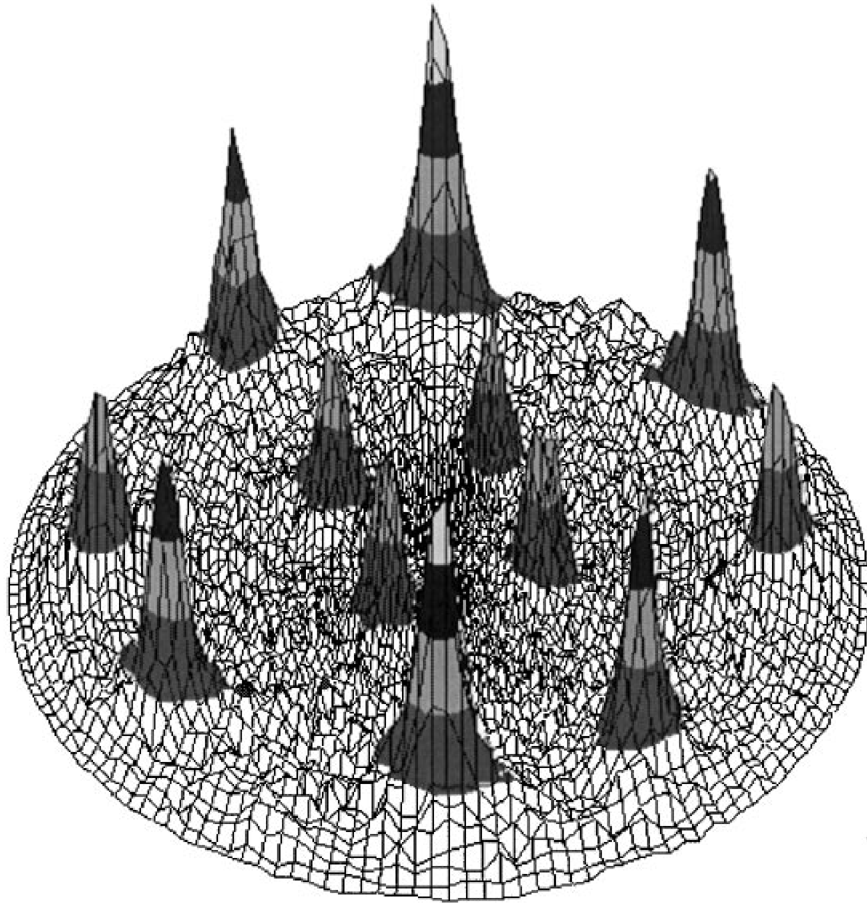

Figure 5 XRD pole figure: $\{1\,1\,3\}$ γ-Ga_2O_3, $2\theta = 36^\circ$.

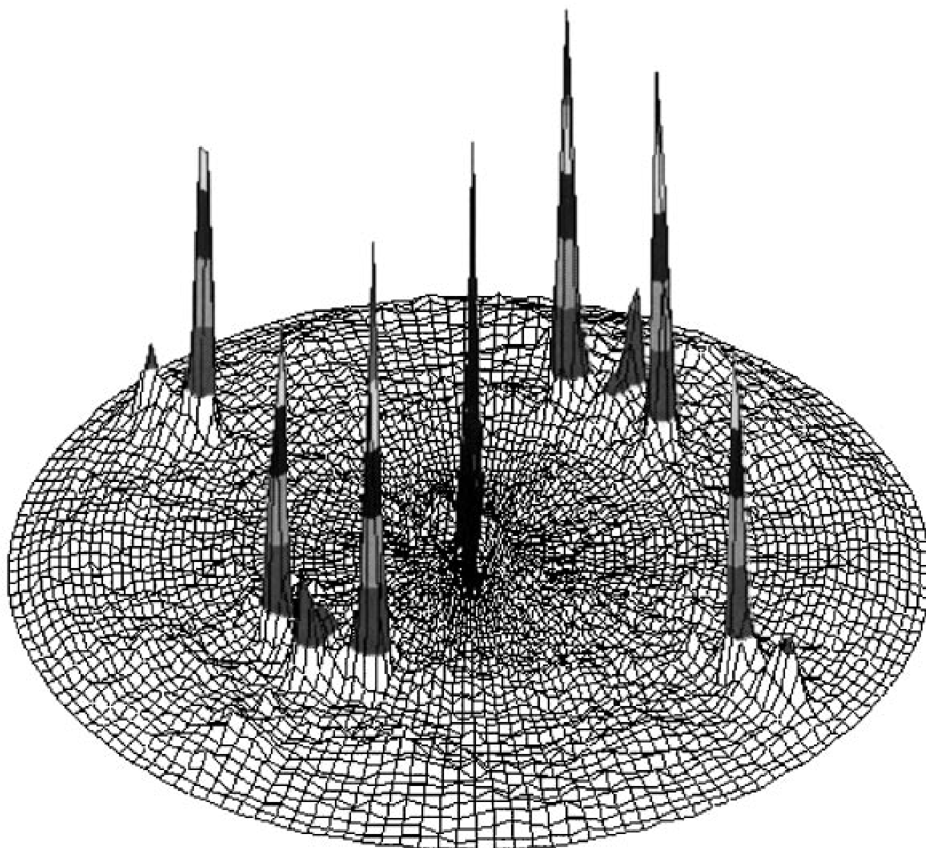

Figure 6 XRD pole figure: $\{0\,1\,2\}$ As, $2\theta = 32.4^\circ$.

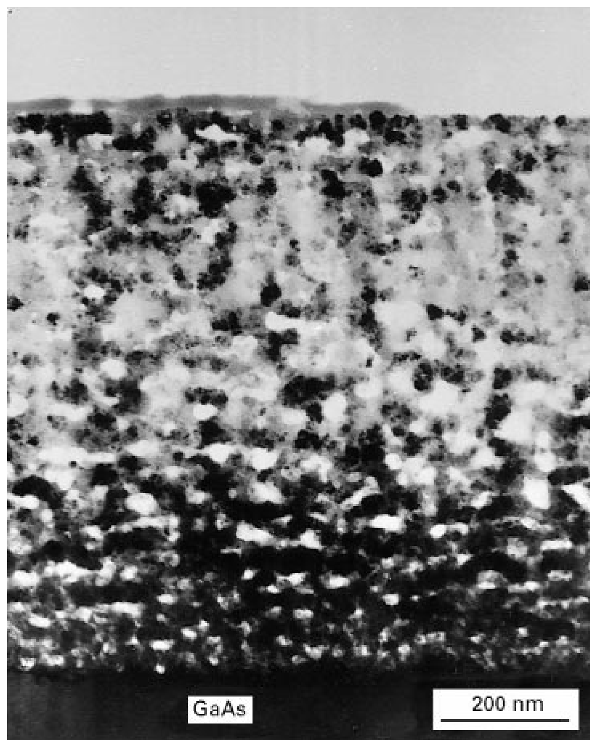

Figure 7 TEM cross-section bright-field image of the GaAs surface in a macro bubble.

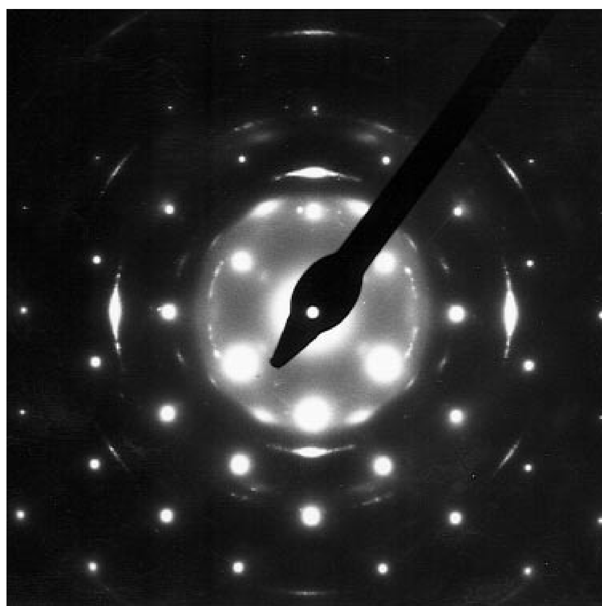

Figure 8 TEM electron diffraction image of the porous material at the GaAs surface in a macro bubble.

wafers. A high pressure up to the range of 10^8 Pa can develop in small bubbles during heating of bonded silicon wafers. The phase γ-Ga_2O_3 is known to be formed under hydrothermal conditions. Pohl [17] reacted metallic gallium with an aqueous solution of ethylene diamine at a temperature of 150 °C and a pressure of 5×10^5 Pa. After several days of heating a fine-grained powder of γ-Ga_2O_3 was obtained. The high water pressure arising during heating of the bonded GaAs and sapphire wafers is most likely responsible for the formation of γ-Ga_2O_3 instead of the low pressure phase β-Ga_2O_3.

4. Conclusions

Chemical composition and crystal structure of phases grown at the interface of GaAs directly bonded to sapphire were identified. A high density of micro bubbles filled with amorphous or randomly oriented material was observed. The composition of these materials deviates from GaAs towards Ga- or As-rich stoichiometries, with only a spurious oxygen content. The macro bubbles are debonded areas filled with porous and textured γ-Ga_2O_3 and with well-oriented elemental arsenic. While arsenic oxides grown immediately are unstable, the thermodynamically stable γ-Ga_2O_3 collects all the excess oxygen at the interface and leads to the formation of macro bubbles. A network of micro channels is a residuum of the material transport during the formation of the macro bubbles.

Acknowledgement

We want to thank N. D. Zakharov for high resolution TEM investigations.

References

1. C. HUNT, H. BAUMGART, S. IYER, U. GÖSELE and T. ABE (eds), Proceedings of the 3rd International Symposium on Semiconductor Wafer Bonding: Science, Technology and Applications (Electrochem. Soc., Pennington, NJ, 1995).
2. S. BENGTSSON, *J. Electr. Mater.* **21** (1992) 669.
3. T. STENGL, K.-L. AHN and U. GÖSELE, *Jpn. J. Appl. Phys.* **27** (1988) 2364.
4. U. GÖSELE, M. REICHE and Q.-Y. TONG, *Microelectr. Engng* **28** (1995) 391.
5. J. HAISMA, *Philip J. Res.* **49** (1995) 171.
6. D. I. BABIC, J. J DUDLEY, K. STREUBEL, R. P. MIRIN, J. E. BOWERS and E. L. HU, *Appl. Phys. Lett.* **66** (1995) 1030.
7. R. J. RAM, L. YANG, K. NAUKA, Y. M. HOUNG, M. LUDOWISE, D. E. MARS, J. J. DUDLEY and S. Y. WANG, *ibid.* **62** (1993) 2474.
8. J. SÖDERKVIST (ed.), in "Mirco Structure Bulletin", Newsletter for Scandinavian Micro Structure Technology, Uppsala University Sweden, **1** (1995).
9. H. LEMME, *Elektronik* **20** (1996) 42.
10. H. L. HARTNAGEL, in "Properties of gallium arsenide", 2nd edition (INSPEC, London 1990), p. 369.
11. A. YAMADA, M. OASA, H. NAGABUCHI and M. KAWAHIMA, *Mater. Lett.* **6** (1988) 167.
12. Z. L. LIAU and D. E. MULL, *Appl. Phys. Lett.* **56** (1990) 737.
13. M. E. GRUPEN-SHEMANSKY, G. W. HAWKINS and H. M. LIAW, in Proceedings of the 1st International Symposium on Semiconductor Wafer Bonding: Science, Technology and Applications, Phoenix, AZ, October 1991, edited by U. Gösele, T. Abe, J. Haisma and M. A. Schmidt (Electrochem. Soc., Pennington, NJ, 1992), p. 132.
14. P. KOPPERSCHMIDT, ST. SENZ, G. KÄSTNER, D. HESSE and U. M. GÖSELE, in Proceedings of the 23rd International Conference on Physics of Semiconductors (ICPS), Berlin, June 1996, edited by M. Scheffler and R. Zimmermann (World Scientific Publishing, Singapore, 1996) p. 967.
15. W. P. MASZARA, G. GOERTZ, A. CAVILLA and J. B. McKNITTERICK, *J. Appl. Phys.* **64** (1988) 4943.
16. K. MITANI and U. M. GÖSELE, *Appl. Phys. A* **54** (1992) 543.
17. K. POHL, *Naturwissenschaften* **55** (1968) 82.

Received 2 January
and accepted 17 December 1997